Assemblages and chemical composition of amphiboles in rocks of the Jílové Belt, Central Bohemia

Asociace a chemické složení amfibolů hornin Jílovského pásma, střední Čechy (Czech summary)

(7 text-figs, 2 plates, 4 tabs)

EVA FEDIUKOVÁ[1] – FERRY FEDIUK[1]

[1] *Geohelp, Na Petřinách 1897, Praha 6, Czech Republic*

Amphiboles constitute, along with feldspars and quartz, the most widespread minerals of the Proterozoic metavolcanic Jílové Belt. They occur in major amount in its metabasaltic and metaandesitic rocks, but they are locally also present as a characteristic subordinate constituent in acid members of the belt, namely in orthogneisses. Many species of amphiboles can be distinguished here: dominant magnesiohornblende, abundant actinolite and less common tschermakite, ferrotschermakite, ferrohornblende, ferroactinolite, pargasite, ferropargasite and edenite. Cummingtonite is widespread. In contrast, typical alkali amphiboles and NaCa amphiboles are absent. In most samples, two up to four of the above mentioned species usually occur. The present assemblages resulted from an interaction of the bulk rock chemistry with pre-Palaeozoic regional and Variscan contact metamorphism. Relictic amphiboles of the magmatic stage, represented by high-alumina members, are present in subordinate amount only.

Key words: amphiboles, electron microprobe, metamorphism, Proterozoic, volcanics, Bohemian Massif

Introduction

The Jílové Belt (JB), named by Kettner (1914) after an old mining town situated in its NNE promontory, is an arched, 65 km long and only 1–5 km wide strip of Proterozoic volcanic and subvolcanic rocks. The present understanding of the geology of the JB is based on modern investigation summarised by Morávek et al. (1991) and a detailed geological map 1:25 000 (Morávek et al. 1994). The diversified magmatic lithology of the JB was largely modified to various degrees by hydrothermal, regional and contact metamorphism. The compositional range of JB metavolcanics is very broad, mostly of subalkaline character, comprised of metabasalt (see Plate 1), basaltic metaandesite, metaboninite, metaandesite, metadacite and metarhyolite with a subordinate extension to a slightly alkaline series (basaltic trachyandesite and trachyandesite). Subvolcanic members are classified as leucocratic albite metagranite, orthogneiss (see Plate 2), metatonalite and metagabbro. The strong predominance of Na is the most prominent feature for the whole JB lithology. Geological sketch map of the JB is shown in Fig. 1. The frame of the JB consists of Proterozoic, partly also of Early Palaeozoic sediments and of Variscan granitoids.

In the present contribution, we intend to broaden the meagre analytical data published to date for the JB amphiboles, and to test the variation of their distribution along the belt.

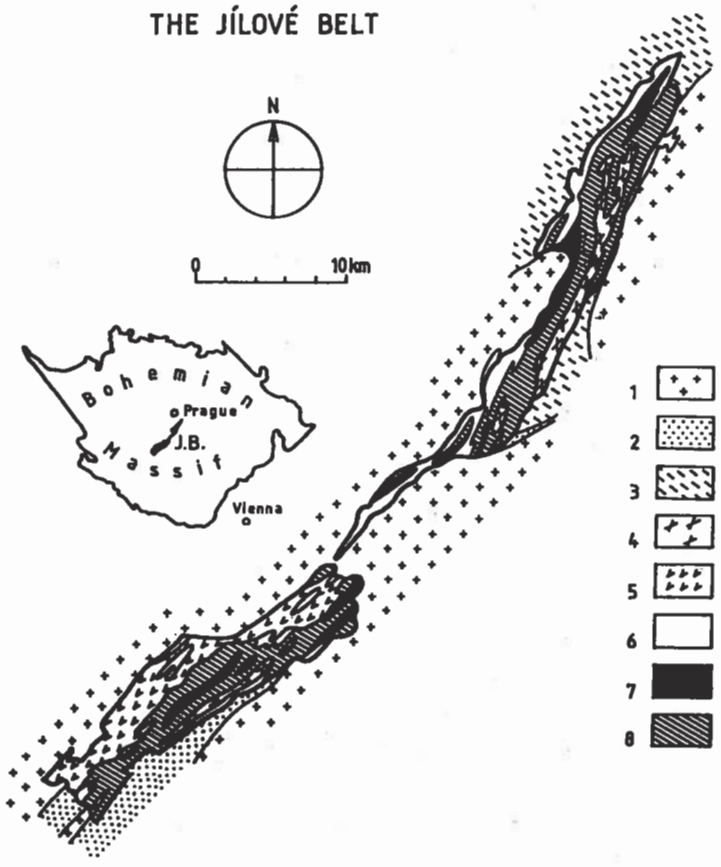

Fig. 1. Geological sketch map of the Jílové Belt. 1 – Central Bohemian granitoid pluton, 2 – Early Palaeozoic metasediments, 3 – Proterozoic metasediments, 4 – albite metagranite, 5 – orthogneiss, 6 – metarhyolite, 7 – metadacite, 8 – metaandesite and metabasalt.

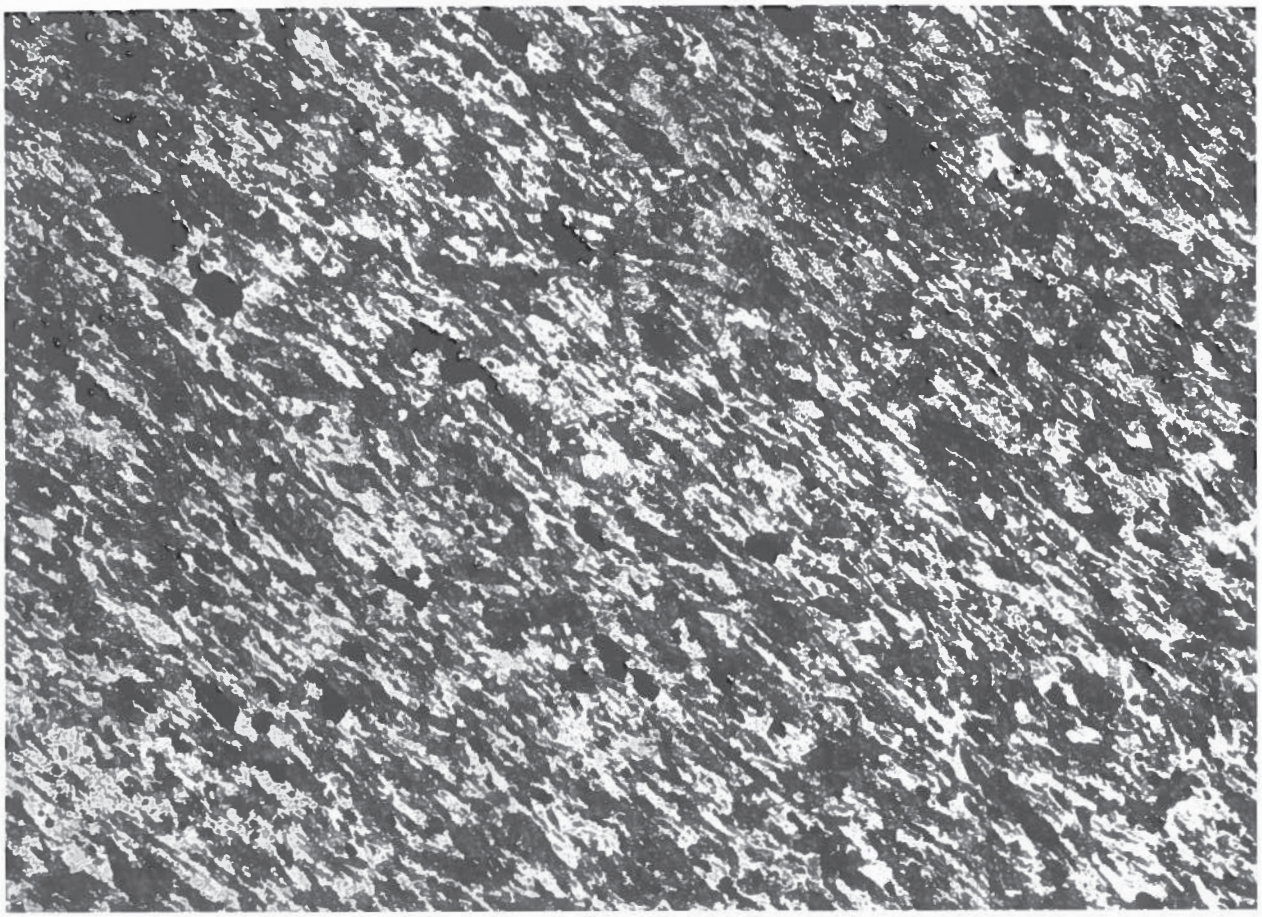

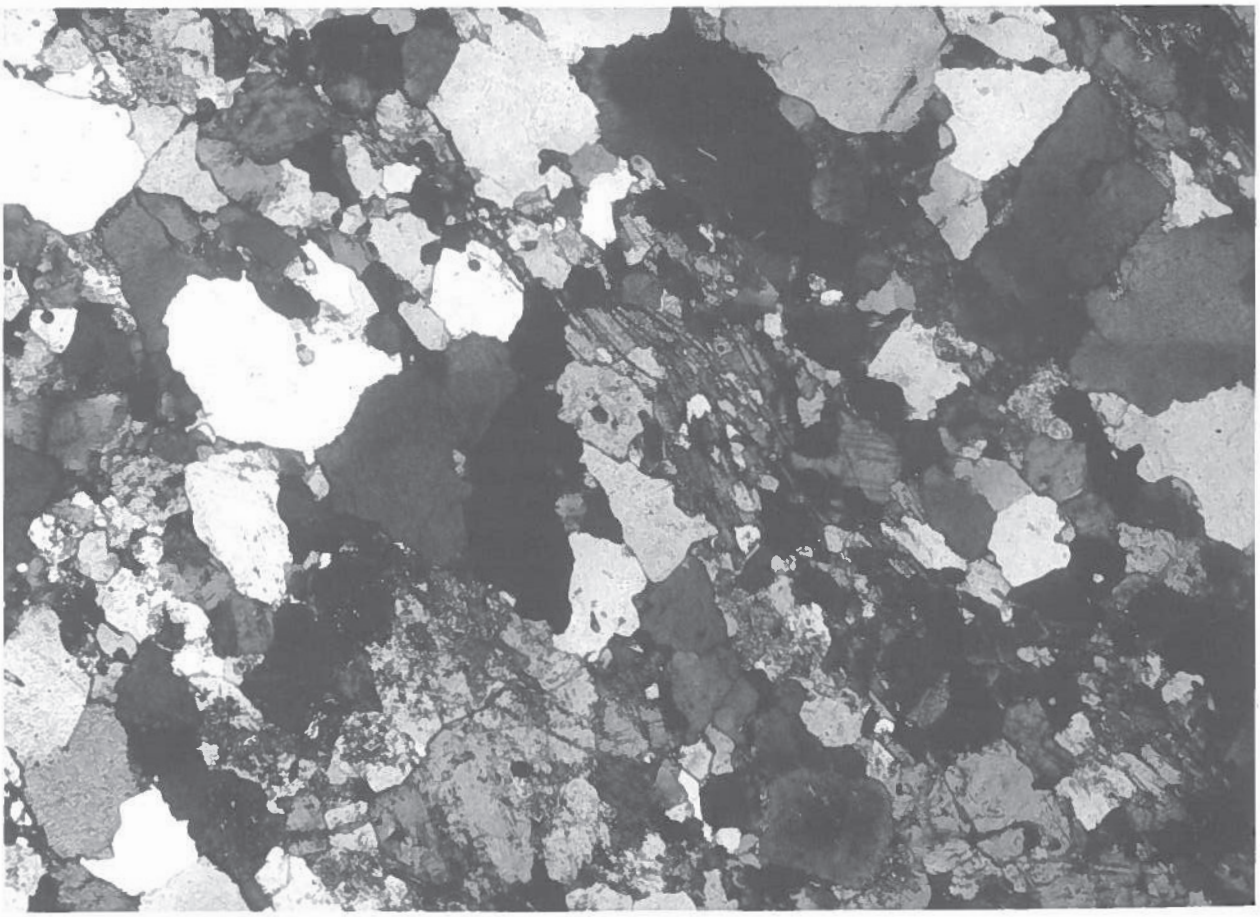

⇦

Plate 1. Typical amphibole-rich metabasite of the Jílové Belt. Left bank of the Vltava-River, 1.5 km downstream from Solenice near the Orlík-dam. Plane-polarised light, enlarged 17.5x.

⇦

Plate 2. Leucocratic amphibole-bearing orthogneiss. Abandoned quarry E of Bor. Crossed polars, enlarged 17.5x.

Field sampling and methods

Thirty fresh samples of JB rocks were collected to assemble a set covering the main amphibole-bearing rock types along the full extent of the belt. Polished thin sections were prepared from all samples and examined in transmitted light. Fifteen most suitable samples (see Fig. 2) were used for electron-microprobe (EMPA) analyses. Most of the analytical work was done in the Laboratory of the Czech Geological Survey in Prague, using the scanning microscope Cam Scan 4 with the energy-dispersing analyser Link Isis (operators Z. Kotrba and I. Vavřín) under following conditions: acceleration 15 kV, current 3 nA, counting time 80 sec., analytical standards for Fe, Mn an Mg – synthetic olivine, Ca – natural wollastonite, Si, Al – natural kyanite and Na, K – natural feldspars. A lesser number of analyses was carried out in the Laboratory of Institute of Technology in Tbilisi, equipped with the Camebac scanning microscope (operator D. M. Shengelia).

Petrography

The set of 15 samples examined and their localities are shown in Table 1. Their short petrographic characteristics are as follows (minerals arranged by decreasing abundance):

1 – Greyish green schistose fine-grained rock with faint layering: amphibole (3 types), > oligoclase > epidote > chlorite >> quartz > titanite.

2 – Bluish grey-green schistose fine-grained rock: oligoclase > amphibole (3 types) > quartz > opaque phases.

3 – Dark grey-green fine- to medium-grained rock with faint schistosity: amphibole (4 types) > andesine > opaque phases > epidote ≡ chlorite > quartz, (apatite).

4 – Dark grey-green schistose fine-grained rock: amphibole (3 types) > andesine > opaque phases ≡ epidote > quartz > biotite, (apatite).

5 – Dark grey-green schistose fine-grained rock: amphibole (3 types) ≡ albite-oligoclase > opaque phases > quartz, (K-feldspar).

6 – Weakly schistose fine-grained rock, greyish green with bluish tint: albite + oligoclase > amphibole (4 types) >> chlorite ≡ epidote > opaque phases, (titanite).

7 – Grey-green, comparatively light-coloured fine- to medium-grained rock with variable schistosity: amphibole (4 types) > oligoclase-andesine >> opaque phases > quartz.

8 – Brownish-grey schistose and spotted fine- to medium-grained rock: quartz > labradorite > amphibole (4 types) > biotite > opaque phases.

9 – Comparatively light-coloured grey-green rock, fine-grained, schistose: albite ≡ amphibole (3 types) >> quartz ≡ opaque phases.

10 – Dark grey fine-grained rock with poorly expressed schistosity: amphibole (3 types) > andesine >> opaque phases > quartz, (apatite).

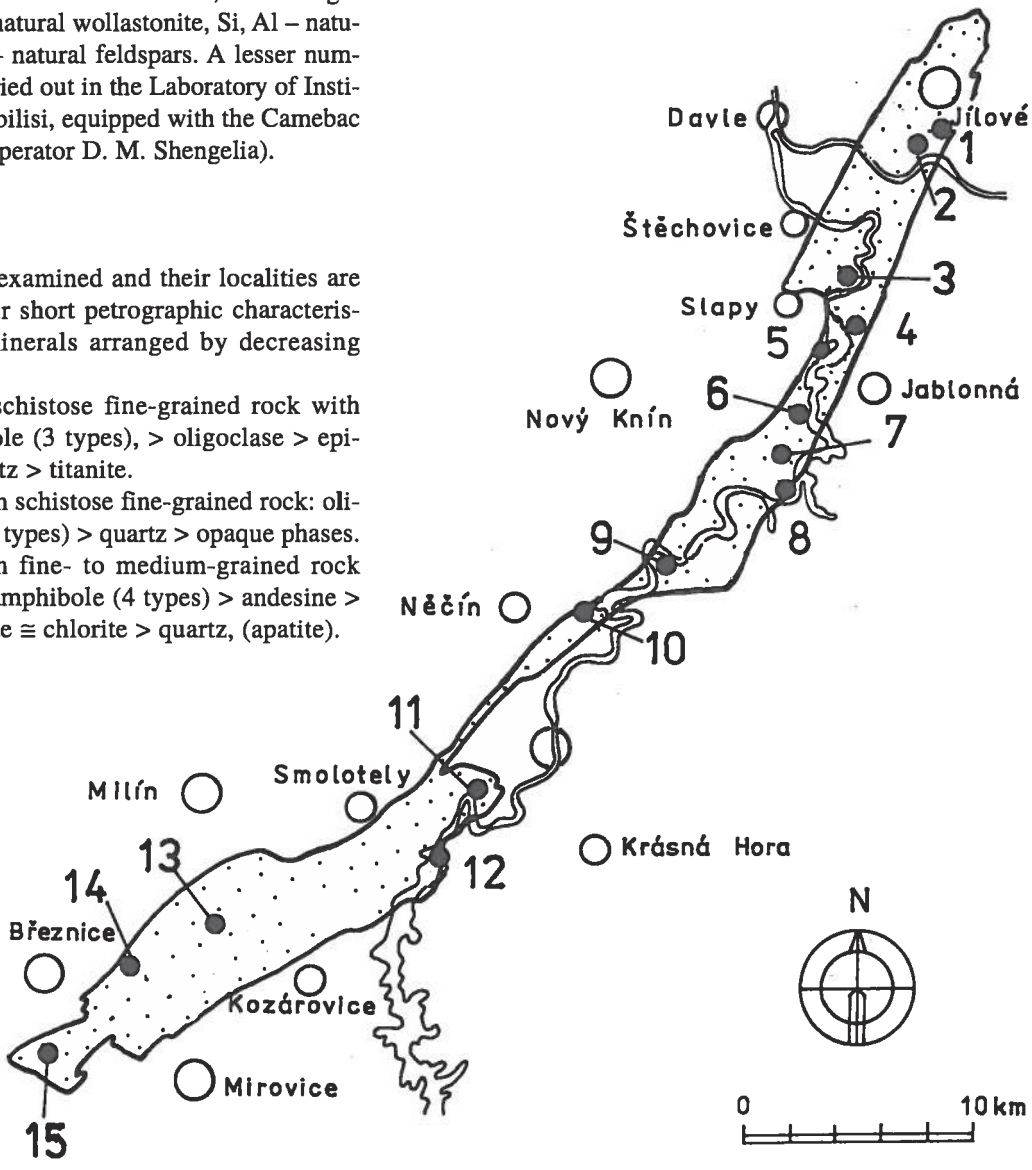

Fig. 2. Contour of the Jílové Belt with the location of analysed samples 1–15.

11 – Greenish grey fine-grained schistose rock: amphibole (4 types) ≅ albite >> chlorite > titanite ≅ quartz > K-feldspar ≅ opaque phases.

12 – Dark greyish-green strongly schistose and fine-grained rock: amphibole (2 types) ≅ oligoclase >> opaque phases > quartz ≅ chlorite.

13 – Greenish-grey fine-grained and schistose rock: albite ≅ hornblende (4 types) >> chlorite ≅ epidote > quartz > titanite (calcite, opaque phases).

14 – Light-coloured whitish, poorly schistose medium-grained rock: oligoclase-andesine ≅ quartz > K-feldspar >> amphibole (2 types) > biotite, (opaque phases).

15 – Light-coloured, yellowish or brownish poorly schistose, medium-grained rock: oligoclase ≅ quartz > K-feldspar >> biotite ≅ amphibole (2 types), (opaque phases).

Opaque phases are represented in all samples mainly by magnetite, ilmenite and/or pyrite.

Chemical compositions of all 15 rocks are shown in Table 2; see Table 1 for their names according to IUGS - TAS diagram (Fig. 3).

The amphiboles

With the exception of Na-metarhyolites and of their subvolcanic equivalents – albite metagranites, all remaining rocks carry amphiboles in variable proportions. Their volume content in the JB as a whole can be estimated roughly at about 20 volume % with the variation range between 0 to 68 %. Based on microscopic examination alone, Krupička (1950) reported the presence of the following amphibole species: hornblende, actinolite, tremolite, anthophyllite and cummingtonite from which tremolite and anthophyllite we were not able to confirm. Additional main papers dealing with the petrography of the JB rocks (Zoubek 1953, Hejtman 1966, Röhlich 1972, Waldhausrová 1984) mentioned only hornblende and actinolite in general. The first, and so far the only sufficiently detailed identifications of the JB amphiboles, based on electron-microprobe analysis, were provided by Morávek et al. (1989) and Pertoldová (1990). The following types were confirmed in these papers: magnesiohornblende, actinolite, ferrohornblende, ferroactinolite and rare ferrotschermakite. Unfortunately, the rocks containing the above spe-

Table 1. List of analysed samples

No	Map No	Rock type	Locality	% amph
1	95	Metaandesite	Borek – Kabáty, abandoned quarry 30 m W of the railway bridge	36
2	92	Metadacite	Žampach, railway cut between the bridge and the tunnel, km 21,375	30
3	163	Metabasaltic dyke	Nové Třebenice, rocky outcrop 300 m E of the Slapy dam	44
4	182	Metabasalt	road Nová Rabyně – Loutí, Vyhlídka, abandoned quarry	50
5	183	Metaboninite	Ždáň, rocky cape, left Vltava bank 300 m W of the port	38
6	200	Metamugearite	left Vltava bank, outcrop 1.5 km NE of Křeničná	28
7	214	Metaboninite	Hněvšín, outcrop along the road 150 m SE of the village	40
8	517	Basaltic metatuffite	outcrop on the right Vltava bank opposite to Kobylníky	17
9	339	Metaandesite	right Vltava bank, rocky outcrop 100 m W of the Cholín bridge	40
10	376	Basaltic metaandesite	left Vltava bank, outcrop opposite to Zvírotice	42
11	388	Metalatite	left Vltava bank, rocky outcrop 1.5 km NE of Solenice	34
12	414	Metaandesite	Popelíky, right Vltava bank 350 m SSE of the Orlík dam	38
13	448	Metaandesite	Svojšice, abandoned quarry 300 m ESE of the village	37
14	466	Orthogneiss	Bor, 150 m E of the village, abandoned quarry	5
15	492	Orthogneiss	Hradec, el. point 531 E of Hudčice, abandoned quarry on the top of the hill	3

Note: Map numbers refer to the map published by Geoindustria (Fediuk 1991)

Table 2. Chemical compositions of amphibole-bearing rocks

	1	2	3	4	5	6	7	8	9	10	11	12	13	14	15
SiO_2	58.21	61.14	47.21	49.50	51.92	54.07	53.43	67.39	59.46	53.47	53.75	56.97	56.77	73.75	76.80
TiO_2	0.47	0.48	2.79	0.75	0.36	0.99	0.40	0.43	0.26	0.49	0.68	0.41	0.40	0.19	0.08
Al_2O_3	17.24	16.24	14.07	17.93	14.01	16.94	13.64	15.25	14.19	18.86	16.10	14.80	14.44	14.15	13.21
Fe_2O_3	2.31	0.48	5.04	3.52	2.37	5.07	3.06	0.97	0.72	3.74	3.91	1.44	2.23	1.24	0.60
FeO	4.85	5.16	8.13	5.07	7.68	4.17	6.10	4.62	4.65	5.76	4.85	6.40	6.38	0.90	0.45
MnO	0.14	0.24	0.17	0.18	0.19	0.13	0.20	0.13	0.12	0.17	0.14	0.15	0.15	0.02	0.01
MgO	3.36	3.87	7.90	8.09	9.36	4.15	9.03	1.46	7.69	4.55	5.27	7.53	5.78	0.54	0.16
CaO	6.69	4.87	7.61	8.32	5.97	5.57	9.07	4.17	6.15	6.74	5.19	4.27	6.05	2.20	1.35
Na_2O	5.05	4.18	3.14	2.65	4.88	6.99	2.13	1.48	4.36	4.14	4.65	5.37	4.17	4.48	4.34
K_2O	0.03	0.02	0.07	0.89	0.23	0.07	0.15	2.04	0.13	0.35	2.93	0.08	0.05	1.26	1.90
P_2O_5	0.11	0.07	0.50	0.15	0.03	0.08	0.04	0.08	0.03	0.05	0.32	0.03	0.04	0.03	0.01
LOI	0.50	0.32	1.98	1.92	1.66	0.82	1.58	0.98	0.92	0.54	1.18	1.34	2.34	0.64	0.54
total	98.96	98.93	98.61	98.97	98.66	99.05	99.15	99.00	98.68	98.86	98.97	98.79	98.80	99.40	99.45

Analysed by Laboratory of Uranium prospecting, Stráž p. Ralskem. See Table 1 for localities.

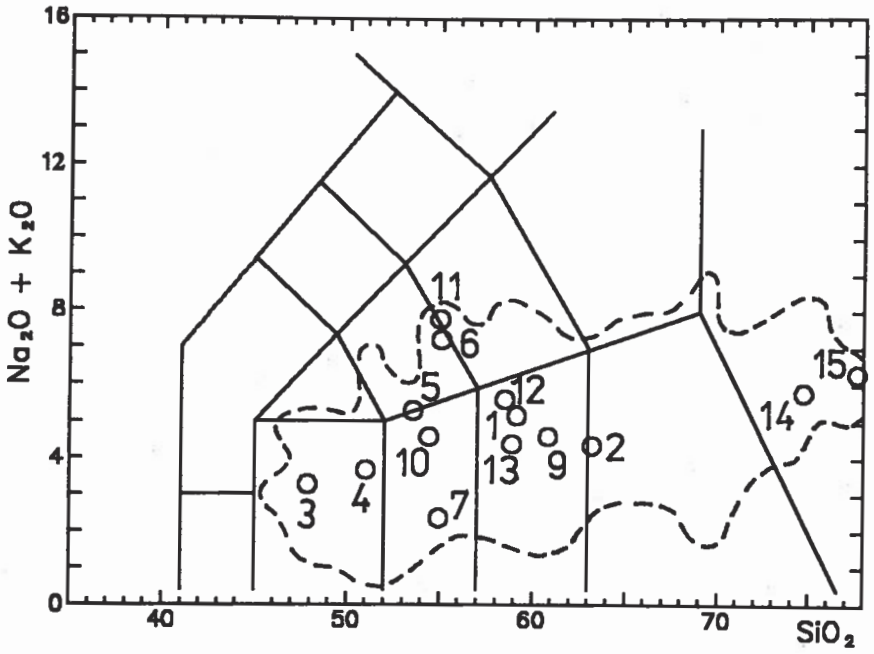

Fig. 3. TAS diagram with plots of the analysed samples 1–15 (sample 8 not included as its origin is mixed, not purely igneous). Dashed contour indicates the range of all JB rocks, based on 524 compositions (in Fediuk et al. 1991). Classification grid after Le Maitre, ed. (1989).

cies do not represent the JB lithologies proper, as they belong to problematic volcaniclastic rocks of the controversial margin of the JB at the gold deposit Mokrsko.

The results of our study are summarised in Table 3 which shows representative compositions of all ten amphibole species identified, selected from the whole set of 80 compositions from 15 rock samples given in Appendix. All compositions were normalised to 23 oxygen equivalents. Ferric and ferrous iron for the total cation charge 46 were balanced using the average of the 15-NK and 13-CNK methods (Richard 1988). For the sake of consistency, this procedure was applied not only to the predominant calcic amphiboles, for which it is the most appropriate method, but also to the subordinate Mg-Fe amphiboles, even when this is not the optimal approach to this category.

The dominant amphibole type in the set of 80 compositions of the Appendix is magnesiohornblende (46.25 % of all compositions), followed by actinolite (21.25 %), cummingtonite (10 %), ferrohornblende (6.25 %), ferrotschermakite and pargasite (5 % each), ferroactinolite and edenite (2.5 % each) and ferropargasite (1.25 %). Tschermakite, which is suspected from optical properties and paragenesis, is not represented in Table 3. Nevertheless, its minor presence in the JB rocks is highly probable. Short characteristics of individual amphibole species are given below.

Magnesiohornblende: this amphibole, mostly in irregularly columnar habit, is by far the most widespread in JB. One substantial reason for this fact is purely formal: the new revised classification of amphiboles (Leake et al. 1997) leaves out the former subcategory of actinolitic magnesiohornblende (Si 7.3 to 7.5). This step is justified by rules of IMA nomenclature but is definitely not the optimal solution for petrographic work, which would prefer a more subtle subdivision to show the genetic evolution in the amphibole series. Out of the total of magnesiohornblende cases, 13.5 % would fall into this subcategory showing the link between magnesiohornblende s. s. and actinolite as the final degradation product of the series, as it is clearly documented in Fig. 4. The new classification of Leake et al. (1997) does not provide any prefixes or modifiers for the broad field of the JB magnesiohornblende, but substantial differences among the members of this category are obvious in any case. Namely, magnesiohornblende from orthogneiss (No. 14 and 15 of Table 3) shows markedly higher Na and K values and the modifier ferrian applies to many compositions. The optical properties, too, indicate that the category of magnesiohornblende is not uniform. This is demonstrated especially by pleochroic colours. Brown tints are rather scarce, but the variation in scale and intensity of green shades is very large. Locally, bluish-green tint is observed which prompted some authors to suspect the presence of alkali amphiboles. Our results do not support this interpretation. Also, our amphiboles with comparatively higher alkali content (series with Na+K higher than 0.5, see below) do not exceed the limit of the calcic amphibole series. Among magnesiohornblende compositions, those from orthogneiss (sample 14 and especially 15) do show elevated alkalis contents (see Fig. 4).

Actinolite is present in most samples. Its chemistry is simple, characterised by low Al and alkalis. Neither prefixes, nor modifiers are required to specify its compositions with the exception of actinolite from orthogneiss (samples 14 and 15) which is ferrian. In thin section, acicular actinolite grows on the termination of columnar hornblende; pale greenish colour is the most typical. The gradual evolution of actinolite from magnesiohornblende has been stressed by most authors dealing with the JB.

Cummingtonite its presence in the JB rocks is more common than supposed to date. It was found in basic to intermediate metavolcanics throughout the whole extent of the JB. It occurs mostly in needle-like or thin prismatic

Table 3. Representative compositions of ten EMPA-analysed amphibole species and their crystal-chemical formulae.

	4a	12c	3g	2c	8d	1a	5e	11d	10g	11e
SiO_2	47.66	51.28	55.26	53.78	42.64	39.94	41.85	53.21	47.16	39.75
TiO_2	0.40	0.12	0.15	0.03	0.39	0.13	0.40	0.16	0.74	2.56
Al_2O_3	9.00	5.64	1.64	0.82	13.98	16.75	11.97	0.33	6.50	12.71
FeO	14.02	12.34	11.08	24.09	22.87	24.64	15.16	21.16	16.52	19.50
Cr_2O_3	n. d.	0.09	n. d.	n. d.	0.16	n. d.	0.80	0.19	n. d.	n. d.
MnO	0.23	0.17	tr.	1.30	0.44	0.063	tr.	0.39	0.32	0.36
MgO	12.93	15.04	16.25	16.37	3.76	3.77	11.25	10.29	12.20	7.97
CaO	12.35	12.39	12.47	0.92	10.42	10.35	11.09	12.53	11.07	11.91
Na_2O	0.94	0.82	0.44	0.25	1.05	1.30	2.66	0.07	1.77	1.93
K_2O	0.13	0.02	tr.	0.03	0.38	0.49	0.16	tr.	0.81	1.37
total	97.66	97.91	97.29	97.59	95.99	98.00	95.34	98.33	97.09	98.06
TSi	6.922	7.354	7.935	7.459	6.614	6.069	6.347	7.929	7.052	6.080
TAl	1.078	0.646	0.065	0.085	1.386	1.931	1.653	0.058	0.948	1.920
TFe_3	0.000	0.000	0.000	0.456	0.000	0.000	0.000	0.004	0.000	0.000
TTi	0.000	0.000	0.000	0.000	0.000	0.000	0.000	0.018	0.000	0.000
Sum_T	8.000	8.000	8.000	8.000	8.000	8.000	8.000	8.010	8.000	8.000
CAl	0.462	0.306	0.213	0.049	1.167	1.067	0.485	0.000	0.197	0.369
CCr	0.000	0.010	0.000	0.000	0.020	0.000	0.096	0.22	0.000	0.000
CFe_3	0.323	0.176	0.000	0.848	0.222	0.690	0.379	0.000	0.264	0.173
CTi	0.044	0.013	0.016	0.003	0.046	0.015	0.046	0.000	0.083	0.295
CMg	2.800	3.215	3.479	3.385	0.869	0.854	2.544	2.286	2.720	1.817
CFe_2	1.358	1.270	1.293	0.644	2.648	2.334	1.452	2.633	1.716	2.321
CMn	0.014	0.010	0.000	0.071	0.029	0.40	0.000	0.049	0.020	0.024
CCa	0.000	0.000	0.000	0.000	0.000	0.000	0.000	0.010	0.000	0.000
Sum_C	5.000	5.000	5.000	5.000	5.000	5.000	5.000	5.000	5.000	5.000
BMg	0.000	0.000	0.000	0.000	0.000	0.000	0.000	0.000	0.000	0.000
BFe_2	0.022	0.035	0.038	0.846	0.097	0.107	0.093	0.000	0.086	0.000
BMn	0.014	0.010	0.000	0.081	0.029	0.041	0.000	0.000	0.020	0.022
BCa	1.922	1.904	1.919	0.137	1.732	1.685	1.802	1.991	1.774	1.952
BNa	0.042	0.051	0.044	0.031	0.143	0.167	0.105	0.009	0.120	0.026
Sum_B	2.000	2.000	2.000	1.095	2.000	2.000	2.000	2.000	2.000	2.000
ACa	0.000	0.000	0.000	0.000	0.000	0.000	0.000	0.000	0.000	0.000
ANa	0.223	0.177	0.079	0.036	0.173	0.216	0.677	0.011	0.393	0.547
AK	0.024	0.004	0.000	0.005	0.075	0.095	0.031	0.000	0.155	0.267
Sum_A	0.247	0.180	0.079	0.041	0.248	0.311	0.708	0.011	0.547	0.814

4a – magnesiohornblende with low TSi, 12c – magnesiohornblende with high TSi (= actinolitic magnesiohornblende according to former classification), 3g – actinolite, 2c – cummingtonite, 8d – ferrohornblende, 1a – ferrotschermakite, 5e – pargasite, 11d – ferroactinolite, 10g – edenite, 11e – ferropargasite. Numbering of compositions is identical to that of the complete set of 80 analyses in the Appendix.

form, it is pale yellowish in colour, and commonly shows polysynthetic twinning. The presence of its orthorhombic equivalent - anthophyllite, mentioned by Krupička (1950), was not confirmed. From crystal-chemical point of view (Fig. 5), the prefix ferri belongs to all 8 cummingtonite cases given in the Appendix; one of them is also calcian.

Ferro-series of calcic amphiboles (ferrotschermakite, ferrohornblende and ferroactinolite) is much less represented in comparison with the above- described magnesio-series. Occurrences of these amphiboles are limited to samples No. 1, Nos. 9 and 13, but especially to No. 8 (basaltic metatuffite). Ferrotschermakite is specified by the prefix alumino (or close to it); the same holds for ferrohornblende, but not for ferroactinolite compositions. The intensity of their pleochroic colours is obviously higher compared to members of the magnesio-series, being understandably most intensive for ferrotschermakite (brown shades).

Amphiboles of the high-alkali calcic series $Na+K \geq 0.5$ (pargasite, edenite and ferropargasite) are scarce (7 cases), confined to samples Nos. 4, 5 and No. 11 (Fig. 6). They commonly display elevated contents of Ti (prefix titanian); sample No. 11 also shows high K (prefix potassian). Their pleochroism ranges from yellowish (X) and green-brown (Y) to emerald green (Z).

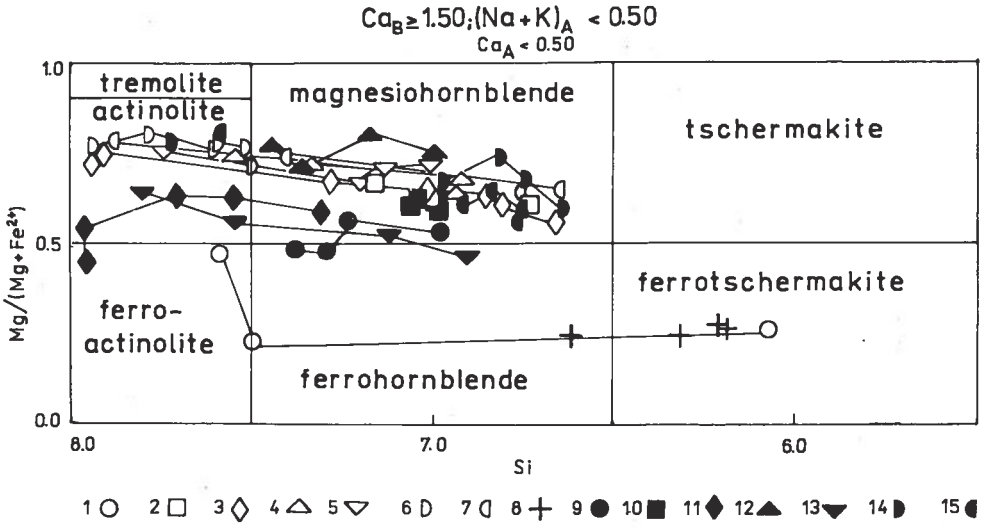

Fig. 4. Classification diagram according to Leake et al. (1997) for calcic amphiboles with $(Na+K)_A < 0.50$. Symbols 1 to 15 correspond to numbering of localities in Fig. 2 and Table 1.

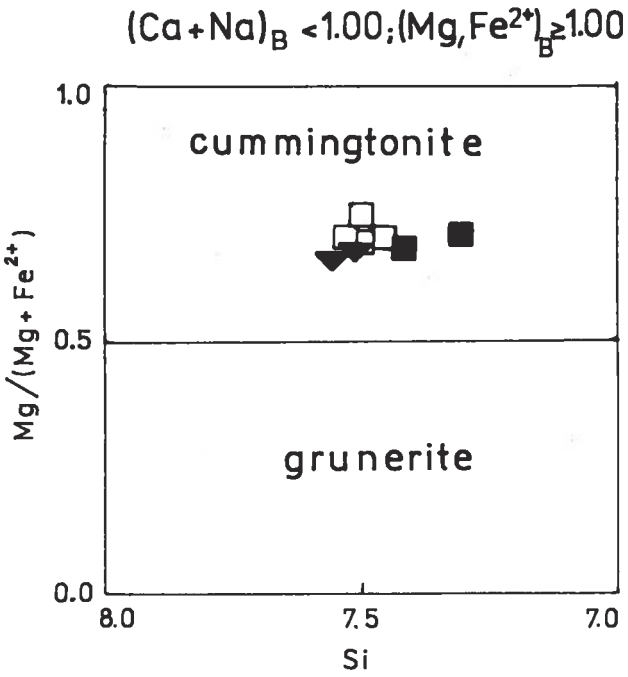

Fig. 5. Classification diagram for cummingtonite and grunerite according to Leake et al. (1997) with representative plots of cummingtonite compositions referred to in the Appendix. For related symbols see Fig. 4.

Figure 7 shows variations of selected oxide contents in the amphiboles examined. Individual amphibole types are clustered with minimal, if any, overlaps. Cummingtonite plots in Fig. 7a and 7b are conspicuously separated from all other categories. In all three diagrams, two amphibole groups occupy the extremes of the non-cummingtonitic amphibole line-ups: the first, characterised by high SiO_2, MgO and CaO and low Al_2O_3, FeO and Na_2O contents, is represented by actinolite and ferroactinolite; the other one, populated by ferrotschermakite, ferrohornblende and in part by pargasite and ferropargasite shows exactly opposite properties. As a conspicuous feature of calcic amphiboles of the JB, the narrow range of CaO contrasting with large scatter of Na_2O values should be pointed out.

We tried to examine the relation between the chemical composition of amphiboles and their position along the length of the JB but the trends in this respect are almost insignificant. Otherwise, a slight decrease in Na+K can be observed in amphiboles from the metavolcanics, whereas the content of alkalis is substantially higher in magnesiohornblende of the orthogneisses in accord with the entirely different bulk composition of these acid rocks. A similar relationship holds for Al^{IV}.

Discussion

Some authors (e. g. Zoubek 1953) emphasized an overall low "epizonal" metamorphism of the JB. Such interpretation was apparently supported by the presence of well-preserved relictic volcanic structures such as pillow lavas, amygdules in basic members and volcanodetritic fabric in acid lithologies, especially in the NE part of the belt. Nevertheless, the mineral assemblages in most JB rocks in general, and the results of our amphibole study in particular, are not consistent with low-grade metamorphism. On the contrary, only a few samples can be ranked with greenschist facies. Most of our green and ostensibly schistose rock samples contain hornblende, with or without actinolite. Moreover, plagioclase associated with this hornblende is represented only locally by albite. More commonly it is oligoclase or even more calcic plagioclase as determined optically as well as by EMPA. Thus, the most widespread regional metamorphic assemblages in the JB, hornblende + oligoclase, and andesine + epidote, could be considered as a metastable transition between lower amphibolite (always without almandine) and the incipient albite-epidote facies.

As stressed by Morávek – Röhlich (1971), Röhlich (1972) and Fediuk et al. (1991), the metamorphic framework is complicated by a strong contact metamorphism during the intrusion of Variscan (Carboniferous) granitoids, which followed the pre-Palaeozoic regional metamorphism. Krupička (1950) erroneously connected such thermal effects with the intrusive activity of JB itself. He as-

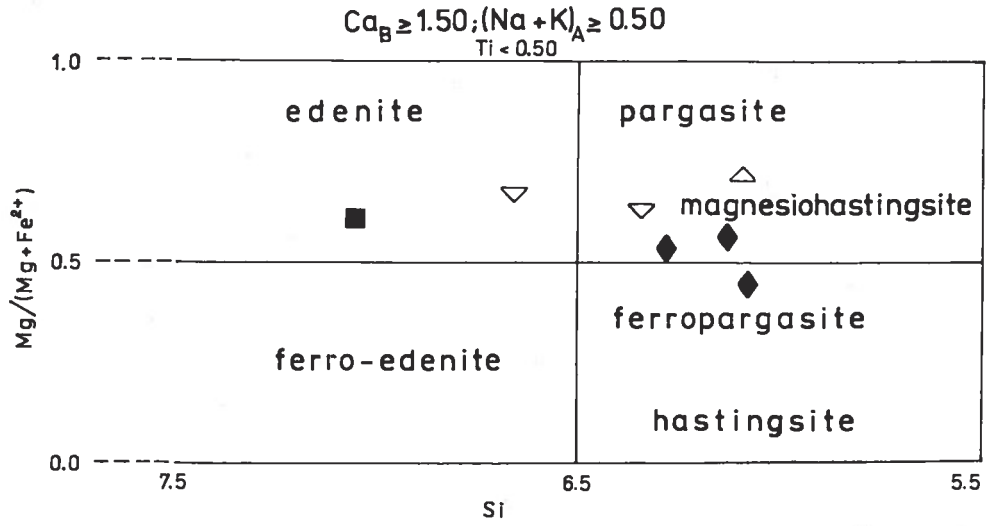

Fig. 6. Classification diagram according to Leake et al. (1997) for calcic amphiboles with $(Na+K)_A \geq 0.50$). For symbols see Fig. 5.

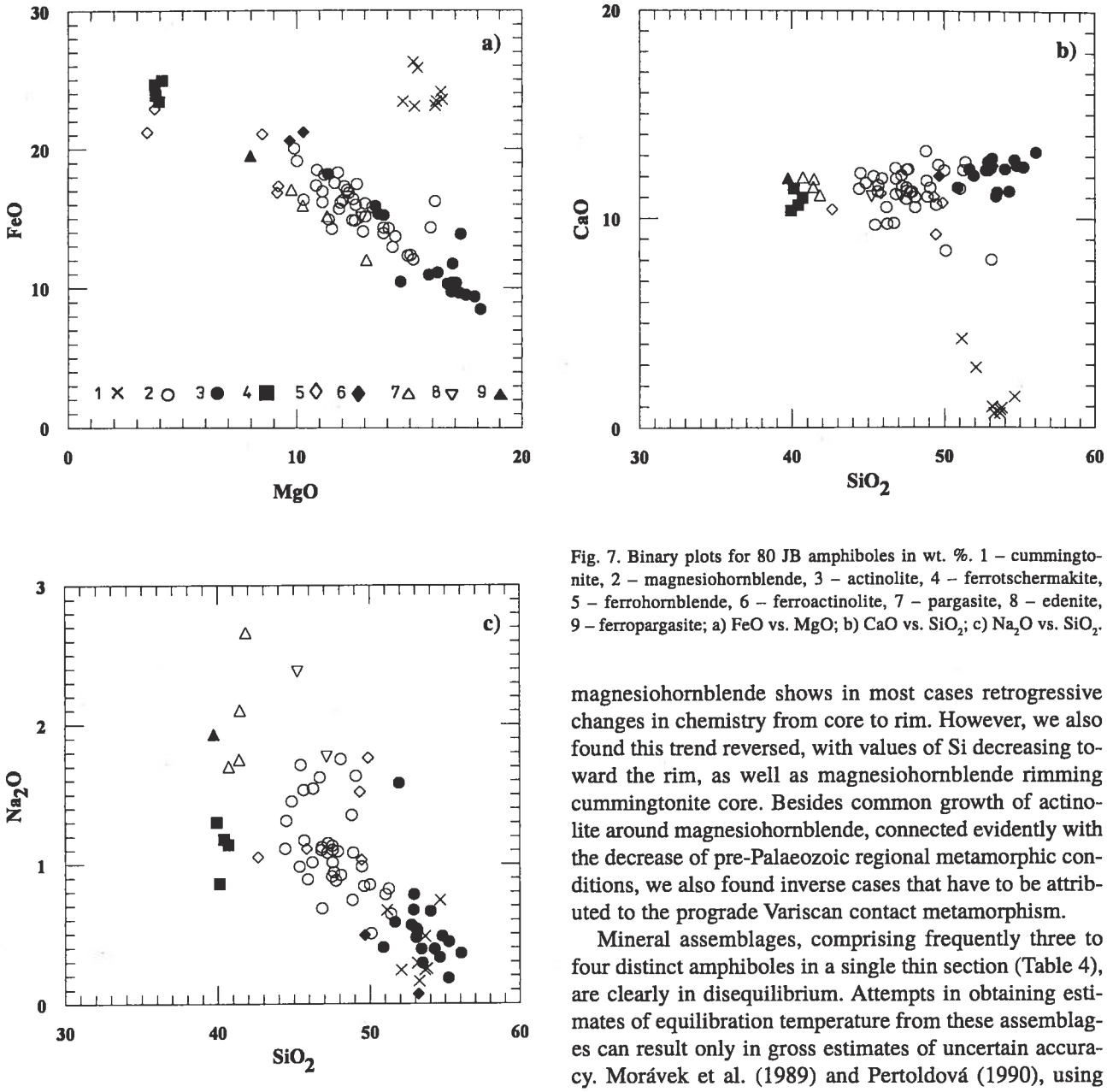

Fig. 7. Binary plots for 80 JB amphiboles in wt. %. 1 – cummingtonite, 2 – magnesiohornblende, 3 – actinolite, 4 – ferrotschermakite, 5 – ferrohornblende, 6 – ferroactinolite, 7 – pargasite, 8 – edenite, 9 – ferropargasite; a) FeO vs. MgO; b) CaO vs. SiO_2; c) Na_2O vs. SiO_2.

sumed that the degradation of mineral assemblages, caused by decrease of regional P, T conditions, remained frozen and could not run in the reverse direction during successive temperature rises conditioned by acid magma intrusion. Although metabasites are in general relatively insensitive to the effects of contact metamorphism, the statement of Krupička (1950) cannot be correct. Krupička's interpretation is contradicted not only by observations of Tracy – Frost (1991) on contact metamorphism of mafic rocks, but also by the evidence gleaned directly from the JB: Hejtman (1966) described here a prograde contact metamorphic transformation of a JB metabasite into hypersthene – amphibole – plagioclase – magnetite hornfels directly at the contact with a granitoid body. Large-scale effects of Variscan contact metamorphism, which established the final and dominant amphibole-hornfels and epidote-amphibole-hornfels facies, were proved for the northern part of the JB by Röhlich (1972). In our EMPA study, magnesiohornblende shows in most cases retrogressive changes in chemistry from core to rim. However, we also found this trend reversed, with values of Si decreasing toward the rim, as well as magnesiohornblende rimming cummingtonite core. Besides common growth of actinolite around magnesiohornblende, connected evidently with the decrease of pre-Palaeozoic regional metamorphic conditions, we also found inverse cases that have to be attributed to the prograde Variscan contact metamorphism.

Mineral assemblages, comprising frequently three to four distinct amphiboles in a single thin section (Table 4), are clearly in disequilibrium. Attempts in obtaining estimates of equilibration temperature from these assemblages can result only in gross estimates of uncertain accuracy. Morávek et al. (1989) and Pertoldová (1990), using amphibole – plagioclase thermobarometers, derived for the JB margin at Mokrsko T = 500–630 °C, P ≤ 400 MPa. Our data for amphibole – plagioclase pairs, applying geothermometer of Blundy – Holland (1990), gave substantially larger span of temperatures (assuming P ≅ 200 MPa). For example, four amphibole species in the metaboninite No 5 at Ždáň show T = 795 °C for pargasite No 5e, 740 °C for edenite No 5f, 615 °C for magnesiohornblende No 5b and 475 °C for actinolite No 5d, the first three coexisting with oligoclase An 13.9, the last one with albite An 5.1. The highest T values were found for ferrotschermakite of sample 1 (metaandesite at Borek – Kabáty with labradorite An 68.5), = 1040 °C, and of sample 8 (basaltic metatuffite opposite to Kobylníky with labradorite An 59.0) = 995 °C. In terms of decreasing temperature, ferrotschermakite is followed by ferrohornblende (890 °C in basaltic metatuffite No 8 opposite to Kobylníky), then by ferropargasite (850 °C in metalatite No 11 at Solenice), pargasite (825 °C

in metalatite No 11 at Solenice, 805 °C in metabasalt No 4 near Nová Rabyně, and 795 °C in metaboninite No 5 at Ždáň) and edenite (740 °C in metaboninite No 5 at Ždáň). Temperatures for magnesiohornblende are split into two separate categories. The category with higher T occurs in orthogneisses No 14 and 15 (790° and 815 °C, respectively), whereas metavolcanics of all types (Nos 2, 4, 5, 10 and 11) show a wide interval of lower T, ranging from 750° to 580 °C. Cummingtonite in samples No 2 and 10 is characterized by T approx. 20 °C lower than coexisting magnesiohornblende. The lowest T (max. 505 °C in metamugearite No 6 at Křeničná, but dropping deep below under 500 °C in, e. g., samples No 5 and 11) were found for actinolite, always associated with almost pure albite (An 1.5 to 5.1).

Two-feldspars geothermometry of Fuhrmann – Lindsley (1988) gave T = 430 °C in metalatite No 11 at Solenice and 455 °C in metaboninite No 5 opposite to Kobylníky, but 645 °C in ortogneiss No 14 of Bor and 685 °C in orthogneiss No 15 of the Hradec-hill. The responsibility for the conspicuous difference between these two groups of data can be attributed mainly to the character of K-feldspar, which corresponds to low-temperature adularia-type feldspar in metavolcanics No 5 and 11, and to microcline with substantially higher Ca and Na contents in orthogneisses No 14 and 15.

Table 4. Summary of amphibole species and of their distribution

	1	2	3	4	5	6	7	8	9	10	11	12	13	14	15
magnesiohornblende	s	a	a	a	a	s	c		c	a	c	a	s	c	c
actinolite		s	c	c	c	a	c		s		c		c	s	s
cummingtonite		c	c				s			c		c	c		
ferrohornblende			c					c	c				s		
ferrotschermakite	c							a							
pargasite				s	s	c					c				
ferroactinolite	c							s			s				
edenite						c				s					
ferropargasite								s			s				

a = abundant, c = common, s = scarce, empty field = not found; see Table 1 for localities.

which cover a substantial part of the Mg-Fe and calcic (Na < 0.5 as well as Na > 0.5) groups. On the contrary, neither NaCa nor alkali amphiboles were found. The impact of the rock bulk chemistry on the amphibole composition is evident if we compare the group of acid orthogneisses with the predominant group of intermediate and basic metavolcanics: the spectrum of amphiboles in orthogneisses is substantially more restricted and their magnesiohornblende is markedly richer in alkalis. On the other hand, analogous dependences among the metavolcanics are rather poor, despite their chemical diversity. This can be demonstrated, e. g., for cummingtonite. This Ca-poor species occurs in both the Ca-poor as well as the Ca-rich rocks, and the metamorphic environment is responsible for its formation more than the rock chemistry. As far as the compositional changes of amphiboles along the longitudinal profile of the belt are concerned, they do exist, but they are very poorly expressed.

The origin of the amphibole diversity is complicated. A subordinate part of them can be considered as relics of pre-metamorphic magmatic state (ferrotschermakite, tschermakite, probably also ferrohornblende, ferropargasite, pargasite and edenite). However, most of the amphibole species were formed during the pre-Palaeozoic regional metamorphism (magnesiohornblende and cummingtonite) and during the gradual decrease of its intensity (magnesiohornblende with high Si-values and actinolite). Finally, some amphiboles originated during, or were influenced by the contact metamorphism connected with Variscan granitoids (minor part of magnesiohornblende and actinolite and probably also of cummingtonite).

Recently, Ledvinková et al. (1999) published a large set of amphibole compositions from gabbroic sills and megaenclaves in tonalites of the NW margin of the Central Bohemian pluton, in close vicinity of the JB. They consider the character of these amphiboles supporting a close genetic affinity between gabbros of Central Bohemian pluton and of metavolcanics of the JB. Our amphibole data are consistent with such statement, even when some differences cannot be neglected, such as substantially higher Fe/Mg ratio in our cummingtonite relative to that from gabbros of Ledvinková et al. (1999).

Conclusions

Amphiboles are prominent constituents of the Jílové - Belt rocks. They belong to a broad spectrum of species

Acknowledgements. We express our thanks to P. Morávek and P. Röhlich for stimulating discussions concerning the Jílové Belt problems, to M. Novák and J. Waldhausrová for critical reading the manuscript, to P. Černý for prompting us to write this paper and for valuable linguistic help, and to Z. Kotrba, D. M. Shengelia and I. Vavřín for efficient assistance in electron-microprobe analyses.

Submitted December 15, 1999

References

Blundy, J. D. – Holland, J. B. (1990): Calcic amphibole equilibria and a new amphibole-plagioclase geothermometer. – Contr. Mineral. Petrol., 104, 208–224.

Fediuk, F. (1991): Jílovské pásmo, mapa lokalizace chemických analýz 1:25 000. – Geoindustria Praha.

Fediuk, F. (1992): Metaboninite in the Proterozoic Jílové belt of Central Bohemia. – Věst. Ústř. Úst. geol., 67/5, 297–310, Praha.

Fediuk, F. – Schulmann, K. – Holub, F. V. (1990): Jílovské pásmo. Strukturně-petrologická studie. – MS Geofond Praha.

Fediuk, F. – Fatková, J. – Janatka, J. – Waldhausrová, J. (1991): Petrografie jílovského pásma. – MS, App. C3 in Morávek P. et al.: Jílovské pásmo. Geoindustria, 64 pp. + příl., Praha.

Fuhrman, M. L. – Lindsley, D. H. (1988): Ternary – feldspars modelling and thermometry. – Amer. Mineral., 73/3–4, 201–215.

Hejtman, B. (1966): A contribution to the petrography and petrochemistry of the Jílové Zone /Central Bohemia). – Paleovolcanites of the Bohemian Massif, 37–49, Charles Univ., Prague.

Kettner, R. (1914): O povltavských vyvřelinách mezi Svatojánskými proudy a ústím Berounky. – Věst. 5. Sjezdu čes. Přír. a Lékařů, Praha.

Krupička, J. (1950): Metamorfismus ve střední části Jílovského pásma. – Sbor. Stát. geol. Úst. ČR. 17, 1–103, Praha.

Leake, B. E. – Woolley, A. R. – Arps, C. E. S. et al. (1997): Nomenclature of amphiboles: Report of the Subcommittee on Amphiboles of the International Mineralogical Association, Commission on New Minerals and Mineral Names. – Amer. Mineral. 82, 1019–137.

Ledvinková, V. – Waldhausrová, J. – Palivcová, M. (1999): Recrystallized members of Upper Proterozoic ultramafic magmatism in the Variscan felsic/mafic stratified plutonic series in the Teletín quarries (Central Bohemian pluton, Bohemian massif). – Krystalinikum 25, 49–82, Morav. Mus., Brno.

Le Maitre, R. W., ed. (1989): A classification of igneous rocks and glossary of terms. – Blackwell Sci. Publ., 193 pp., Oxford.

Morávek, P. et al. (1991): Závěrečná zpráva Jílovské pásmo. – MS Geofond Praha.

Morávek, P. – Fediuk, F. – Röhlich, P. – Váňa, T. (1994): Jílovské pásmo: geologická mapa 1:25 000 a vysvětlivky. – Gabriel Publ. House, Praha.

Morávek, P. – Janatka, J. – Pertoldová, J. et al. (1989): The Mokrsko gold deposit – the largest gold deposit in the Bohemian Massif, Czechoslovakia. – Econ. Geol., Monograph 6, 252–259.

Morávek, P. – Röhlich, P. (1971): Geology of the northern part of the Jílové zone. – Sbor. geol. Věd, G 20, 101–145, Praha.

Pertoldová, J. (1990): Petrologický výzkum minerálů ložiska Mokrsko. – MS Geoindustria (App. C 3/5 Report Mokrsko-západ), Praha.

Richard, L. R. (1988): Minpet. Mineralogical and petrological data processing system. – Quebec, Canada.

Röhlich, P. (1972): Petrografické poměry v severní části jílovského pásma. – Sbor. geol. Věd G, 22, 7–64, Praha.

Tracy, R. S. – Frost, B. R. (1991): Phase equilibria and thermometry of calcareous, ultramafic and mafic rocks, and iron formations. In *Kerrick, D. M., ed.* (1991): Contact metamorphism. – Review in Mineral., 26. Mineral. Soc. Amer., Chelsea, Mich.

Waldhausrová, J. (1984): Proterozoic volcanics and intrusive rocks of the Jílové zone in Central Bohemia. – Krystalinikum 17, 77–79, Praha.

Zoubek, V. (1953): Geologické podklady k projektu údolní přehrady na Vltavě u Zlakovic. – Geotechnica 15, 165 pp., Praha.

Asociace a chemické složení amfibolů hornin Jílovského pásma, střední Čechy

V metavulkanitech jílovského pásma tvoří amfiboly spolu se živci a křemenem převážnou minerální složku. Podstatnou měrou jsou zastoupeny především v metaandezitových a metabazaltových horninách, vystupují však jako sice nepodstatná, ale velmi příznačná složka i v některých kyselých vyvřelinách, jmenovitě v ortorulách. Druhově jsou značně rozrůzněny. Nejrozšířenějším druhem je magnesiohornblend, častý je aktinolit, dále se však vyskytuje tschermakit, ferrotschermakit, ferrohornblend, ferroaktinolit, pargasit a edenit. Běžně je zastoupen cummingtonit. Chybějí však jak typické alkalické amfiboly, tak i NaCa amfiboly. V jedné a téže hornině se obvykle vyskytují dva až čtyři z výše uvedených druhů. Pozorované asociace amfibolů jsou výsledkem interferencí horninového chemického prostředí a předpaleozoické regionální metamorfózy i variské metamorfózy kontaktní. Reliktní amfiboly magmatického stadia jsou zastoupeny jen v podružném množství.

Appendix: Compositions of 80 EMPA-analysed amphiboles from 15 hand specimens and their classification parameters

	1a	1b	1c	2a	2b	2c	2d	2e	2f	2g	3a	3b	3c	3d	3e	3f
SiO_2	39.94	49.46	49.68	53.16	53.68	53.78	54.67	47.55	48.92	45.67	44.53	47.22	45.38	54.66	46.83	50.03
TiO_2	0.13	0.25	0	0	0.05	0.03	0	0.44	0.28	0.61	0.50	0.15	0.25	0	0.40	0.18
Al_2O_3	16.75	12.23	2.97	0.57	0.54	0.82	2.12	8.14	6.98	10.05	11.01	7.67	9.42	1.37	9.19	5.82
FeO^t	24.64	21.16	20.56	23.53	23.42	24.09	23.10	16.10	15.12	16.92	16.33	14.81	16.14	10.29	15.66	13.89
MnO	0.63	0.54	0.50	1.25	1.48	1.30	0.84	0.39	0.29	0.29	0.10	0.34	0.13	0.21	0.19	0.20
MgO	3.77	3.44	9.69	16.44	16.17	16.37	16.11	11.95	13.04	11.15	10.32	12.58	11.15	16.68	11.88	13.84
CaO	10.35	9.23	12.03	0.98	0.84	0.92	1.47	11.46	11.03	11.28	12.15	12.06	12.01	12.81	12.40	12.30
Na_2O	1.30	1.03	0.49	0.29	0.48	0.25	0.74	1.13	1.08	1.23	1.31	1.08	0.98	0.33	1.10	0
K_2O	0.49	0.36	0	0	0	0.03	0	0	0.10	0	0.23	0.12	0.31	0	0.12	0
Cr_2O_3	0	0	0	0	0.03	0	0	0	0.03	0	0.18	0	0	0	0.13	0.20
Total	98.00	97.34	95.92	96.22	96.21	97.59	99.05	97.16	96.87	97.20	96.66	96.03	95.77	96.35	97.90	96.46
Si	6.69	7.497	7.585	7.470	7.530	7.459	7.500	6.988	7.159	6.725	6.656	7.012	6.806	7.906	6.852	7.281
Ti	0.015	0.029	0	0	0.005	0.003	0	0.049	0.031	0.068	0.056	0.017	0.028	0	0.044	0.020
Fe^3	0.690	0	0.185	1.291	1.281	1.304	1.241	0.403	0.409	0.469	0.251	0.353	0.397	0	0.334	0.227
Fe^2	2.334	2.682	2.441	1.474	1.466	1.496	1.129	1.576	1.442	1.615	1.791	1.486	1.627	1.245	1.582	1.464
Mg	0.854	0.777	2.206	3.444	3.381	3.385	3.295	2.618	2.845	2.448	2.300	2.785	2.493	3.597	2.591	3.002
Ca_A	0	0	0	0	0	0	0	0	0	0	0	0	0	0	0	0
Ca_B	1.685	1.499	1.968	0.148	0.126	0.137	0.216	1.805	1.729	1.780	1.946	1.919	1.930	1.985	1.944	1.918
Na_A	0.216	0.154	0.128	0.042	0.053	0.036	0.105	0.218	0.163	0.320	0.351	0.268	0.248	0.085	0.282	0.196
Na_B	0.167	0.149	0.017	0.037	0.078	0.031	0.092	0.104	0.144	0.117	0.029	0.043	0.037	0.008	0.030	0.044
K_A	0.095	0.070	0	0	0	0.005	0	0	0.019	0	0.044	0.023	0.059	0	0.022	0
Spec.	FeTS	FeHB	FeAC	CUM	CUM	CUM	CUM	MgHB	MgHB	MgHB	MgHB	MgHB	MgHB	ACT	MgHB	MgHB

Appendix *(continued)*

	3g	4a	4b	4c	4d	4e	5a	5b	5c	5d	5e	5f	6a	6b	6c	6d
SiO_2	55.26	47.66	47.57	51.41	52.78	41.47	48.12	48.84	49.11	54.03	41.85	45.24	51.96	52.94	52.92	54.82
TiO_2	0.15	0.40	0.30	0.18	0.36	2.68	0.44	0.14	0.46	0.29	0.40	0.54	0.17	0.14	0.25	0
Al_2O_3	1.64	9.00	8.77	5.68	4.69	13.30	7.51	5.51	6.40	2.23	11.97	9.67	6.51	3.74	3.99	2.10
FeO'	11.08	14.02	14.85	12.30	10.52	12.00	14.26	12.90	14.30	10.35	15.16	15.06	10.42	9.73	10.37	8.49
MnO	0	0.23	0.24	0.26	0.34	0.16	0.30	0.34	0.30	0.14	0	0.24	0.22	0.25	0.14	0.45
MgO	16.25	12.93	12.47	14.91	15.86	13.07	14.07	14.24	13.84	17.07	11.25	12.85	14.60	16.86	16.89	18.17
CaO	12.47	12.35	12.33	12.70	12.31	11.87	10.53	13.22	11.46	12.36	11.09	11.06	12.04	12.31	12.72	12.53
Na_2O	0.44	0.94	1.10	0.64	0.56	2.10	1.75	1.35	1.63	0.66	2.66	2.38	1.58	0.78	0.67	0.48
K_2O	0	0.13	0.22	0.11	0.10	0.53	0.12	0.06	0.11	0.05	0.16	0.20	0	0	0	0
Cr_2O_3	0	0	0	0.21	0	0	0.05	0.52	0.07	0.08	0.80	0.18	0.12	0	0	0
Total	97.29	97.66	97.85	98.40	97.52	97.18	97.15	97.12	97.68	97.26	95.34	97.42	97.62	96.75	97.95	97.04
Si	7.935	6.922	6.940	7.348	7.546	6.099	7.003	7.182	7.156	7.734	6.347	6.659	7.500	7.598	7.513	7.784
Ti	0.016	0.044	0.033	0.019	0.039	0.296	0.048	0.015	0.050	0.031	0.046	0.060	0.018	0.015	0.027	0
Fe^3	0	0.323	0.272	0.147	0.089	0.345	0.526	0.121	0.285	0.088	0.379	0.419	0	0.108	0.138	0.101
Fe^2	1.331	1.380	1.540	1.323	1.169	1.130	1.210	1.465	1.458	1.151	1.545	1.435	1.258	1.060	1.094	0.907
Mg	3.479	2.800	2.712	3.177	3.380	2.866	3.052	3.121	3.006	3.643	2.544	2.820	3.141	3.607	3.575	3.846
Ca_A	0	0	0	0	0	0	0	0.044	0	0	0	0	0	0	0	0
Ca_B	1.919	1.922	1.927	1.945	1.886	1.870	1.642	2.000	1.789	1.896	1.802	1.744	1.862	1.893	1.935	1.906
Na_A	0.079	0.223	0.272	0.148	0.094	0.530	0.304	0.385	0.348	0.127	0.677	0.543	0.369	0.160	0.150	0.082
Na_B	0.044	0.042	0.039	0.029	0.061	0.069	0.190	0	0.112	0.056	0.105	0.136	0.074	0.057	0.035	0.050
K_A	0	0.024	0.041	0.020	0.018	0.099	0.022	0.011	0.020	0.009	0.031	0.038	0	0	0	0
Spec.	ACT	MgHB	MgHB	MgHB	ACT	PAR	MgHB	MgHB	MgHB	ACT	PAR	EDE	ACT	ACT	ACT	ACT

	6e	6f	7a	7b	7c	7d	8a	8b	8c	8d	9a	9b	9c	9d	10a	10b
SiO_2	53.17	56.10	45.69	44.87	51.06	55.24	40.12	40.71	40.41	42.64	47.28	48.87	49.34	49.90	51.14	52.08
TiO_2	0.17	0.17	0.28	0.23	0.58	0.02	0.41	0.29	0.27	0.39	0.47	0.41	0.31	0.31	0.18	0.34
Al_2O_3	3.21	0.64	11.01	11.36	4.86	1.59	15.48	14.72	14.51	13.98	8.33	5.86	8.90	8.87	1.55	1.84
FeO'	9.63	9.38	14.90	14.21	12.01	9.49	23.41	24.94	23.84	22.87	19.10	18.10	17.29	16.83	23.04	23.39
MnO	0.21	0.39	0.23	0.35	0.42	0.22	0.58	0.70	0.57	0.44	0.25	0.26	0.21	0.19	0.67	0.84
MgO	17.21	17.89	11.43	11.57	15.16	17.50	3.97	4.09	3.80	3.76	10.03	11.23	9.20	9.14	15.19	14.68
CaO	12.88	13.18	11.57	11.68	11.42	12.46	11.41	10.97	10.62	10.42	11.54	11.80	11.04	10.75	4.22	2.86
Na_2O	0.52	0.36	1.17	1.45	0.78	0.18	0.86	1.14	1.18	1.05	1.15	0.74	1.52	1.76	0.67	0.24
K_2O	0	0	0.09	0.17	0.08	0	0.57	0.46	0.51	0.38	0.07	0.04	0.05	0.04	0	0.20
Cr_2O_3	0	0	0	0.59	0.35	0.14	0.02	0.09	0.15	0.16	n. d.	n. d.	n. d.	n. d.	0	0
Total	97.00	98.11	96.37	96.48	96.72	96.84	96.83	98.11	95.86	95.99	98.22	97.31	97.86	97.79	96.66	96.47
Si	7.606	7.942	6.748	6.640	7.395	7.880	6.186	6.208	6.311	6.614	6.982	7.238	7.319	7.411	7.309	7.419
Ti	0.018	0.018	0.031	0.026	0.063	0.002	0.048	0.033	0.032	0.046	0.052	0.046	0.035	0.035	0.019	0.036
Fe^3	0.095	0	0.356	0.330	0.298	0.082	0.473	0.662	0.405	0.222	0.326	0.327	0	0	1.393	1.315
Fe^2	1.057	1.111	1.485	1.429	1.157	1.050	2.546	2.514	2.709	2.745	2.034	1.915	2.145	2.091	1.361	1.471
Mg	3.670	3.776	2.516	2.552	3.273	3.721	0.913	0.930	0.995	0.869	2.208	2.479	2.035	2.024	3.237	3.118
Ca_A	0	0	0	0	0	0	0	0	0	0	0	0	0	0	0	0
Ca_B	1.974	1.999	1.831	1.852	1.772	1.904	1.885	1.792	1.777	1.732	1.826	1.872	1.755	1.711	0.646	0.437
Na_A	0.130	0.098	0.245	0.337	0.110	0.025	0.196	0.227	0.239	0.173	0.237	0.144	0.307	0.353	0.097	0.035
Na_B	0.014	0	0.090	0.079	0.109	0.025	0.061	0.110	0.119	0.143	0.093	0.068	0.130	0.153	0.088	0.031
K_A	0	0	0.017	0.032	0.015	0	0.112	0.084	0.102	0.075	0.013	0.008	0.009	0.008	0	0.036
Spec.	ACT	ACT	MgHB	MgHB	MgHB	ACT	FeTS	FeTS	FeTS	FeHB	MgHB	MgHB	FeHB	FeHB	CUM	CUM

Appendix *(continued)*

	10c	10d	10e	10f	10g	11a	11b	11c	11d	11e	11f	11g	12a	12b	12c	12d
SiO_2	46.86	47.53	47.91	47.57	47.16	49.64	51.67	53.09	53.21	39.75	40.73	41.41	49.50	50.12	51.28	53.12
TiO_2	0.84	0.82	0.93	0.90	0.74	0.54	0.48	0.10	0.16	2.56	2.68	2.23	0.27	0.57	0.12	0.11
Al_2O_3	7.32	6.80	6.76	6.99	6.50	4.81	3.25	2.38	0.33	12.71	12.50	11.74	8.36	5.59	5.64	3.56
FeO^t	16.27	16.79	16.37	17.27	16.52	15.95	15.30	15.21	21.16	19.50	15.92	17.06	13.66	14.32	12.34	16.21
MnO	0.44	0.36	0.38	0.38	0.32	0.23	0.26	0.42	0.39	0.36	0.48	0.37	0.13	0.24	0.17	0.27
MgO	12.04	12.31	12.51	12.11	12.20	12.62	13.61	13.85	10.29	7.97	10.27	9.77	14.36	15.93	15.04	16.14
CaO	11.15	10.92	11.27	11.31	11.07	12.56	12.36	12.40	12.53	11.91	11.96	11.49	10.56	8.43	12.39	8.01
Na_2O	1.12	0.91	1.09	1.01	1.77	0.84	0.58	0.47	0.07	1.93	1.70	1.75	0.98	0.50	0.82	0.53
K_2O	0.33	0.37	0.26	0.17	0.81	0.44	0.29	0.17	0	1.37	1.46	1.50	0.05	0.78	0.02	0
Cr_2O_3	0	0	0	0	0	0.42	0	0.10	0.19	0	0.07	0.05	0.03	0.09	0.09	0.21
Total	96.01	96.81	97.48	97.71	97.09	98.05	97.80	98.19	98.33	98.06	97.77	97.37	97.90	96.57	97.91	98.16
Si	6.975	7.022	7.037	6.981	7.052	7.306	7.551	7.708	7.929	6.080	6.133	6.282	7.051	7.178	7.354	7.450
Ti	0.094	0.091	0.103	0.099	0.083	0.060	0.053	0.011	0.018	0.295	0.304	0.254	0.029	0.061	0.013	0.012
Fe^3	0.430	0.548	0.433	0.549	0.264	0.085	0.095	0.087	0	0.173	0.201	0.188	0.582	0.835	0.176	0.923
Fe^2	1.596	1.527	1.577	1.571	1.802	1.897	1.775	1.760	2.633	2.321	1.804	1.977	1.044	0.879	1.305	0.978
Mg	2.672	2.711	2.739	2.649	2.720	2.769	2.965	2.998	2.286	1.817	2.305	2.210	3.049	3.401	3.215	3.375
Ca_A	0	0	0	0	0	0	0	0	0	0	0	0	0	0	0	0
Ca_B	1.778	1.729	1.774	1.778	1.774	1.981	1.935	1.929	1.991	1.952	1.930	1.868	1.624	1.293	1.904	1.204
Na_A	0.205	0.132	0.190	0.169	0.393	0.229	0.130	0.094	0.011	0.547	0.459	0.444	0.137	0.071	0.177	0.074
Na_B	0.118	0.129	0.120	0.118	0.120	0.010	0.035	0.038	0.009	0.026	0.038	0.071	0.134	0.068	0.051	0.070
K_A	0.063	0.070	0.049	0.032	0.155	0.083	0.054	0.031	0	0.267	0.280	0.290	0.009	0.143	0.004	0
Spec.	MgHB	MgHB	MgHB	MgHB	EDE	MgHB	ACT	ACT	FeAC	FePA	PAR	PAR	MgHB	MgHB	MgHB	MgHB

	13a	13b	13c	13d	13e	13f	14a	14b	14c	14d	14e	15a	15b	15c	15d	15e
SiO_2	53.28	53.65	45.84	47.78	50.90	53.43	44.44	45.93	46.88	48.11	54.32	46.23	45.47	46.28	46.73	53.51
TiO_2	0	0.01	0.21	0.12	0.17	0.09	0.49	0.14	0.13	1.28	0.19	1.35	1.52	1.24	1.34	0.12
Al_2O_3	0.19	0.14	8.62	7.03	4.06	2.36	9.89	8.41	7.98	7.03	1.98	7.47	8.56	7.48	7.63	1.21
FeO^t	26.26	25.81	21.02	20.00	18.17	15.87	17.33	17.01	15.79	16.05	11.72	17.43	18.45	18.26	17.52	13.83
MnO	0.76	0.88	0.20	0.33	0.31	0.27	0.41	0.61	0.60	0.52	0.52	0.68	0.80	0.69	0.67	0.33
MgO	15.15	15.34	8.48	9.90	11.41	13.49	10.87	12.24	13.35	13.03	16.91	12.67	10.90	11.83	11.69	17.26
CaO	0.66	0.68	11.20	11.24	11.48	11.06	11.40	11.90	11.89	11.02	11.29	10.52	9.67	9.71	9.75	11.25
Na_2O	0.16	0.24	1.11	0.88	0.40	0.39	1.11	0.89	0.68	0.92	0.39	1.01	1.71	1.54	1.62	0.29
K_2O	0	0.03	0.02	0	0	0	0.96	0.53	0.37	0.31	0.10	0.84	0.99	0.86	0.83	0.06
Cr_2O_3	0	0	0.51	0	0	0.04	n. d.	n. d.	n. d.	n. d.	n. d.	n. d.	n. d	n. d.	n. d.	n. d.
Total	96.46	96.78	97.21	97.28	96.90	97.00	96.90	97.66	97.67	98.25	97.42	98.20	98.07	97.89	97.78	97.86
Si	7.529	7.556	6.902	7.118	7.543	7.800	6.444	6.745	6.809	6.972	7.732	6.757	6.749	6.835	6.910	7.591
Ti	0	0.001	0.024	0.013	0.019	0.010	0.055	0.015	0.014	0.140	0.020	0.148	0.170	0.138	0.149	0.013
Fe^3	1.446	1.416	0.437	0.469	0.265	0.295	0.541	0.808	0.889	0.568	0.385	0.836	0.613	0.696	0.577	0.808
Fe^2	1.657	1.623	2.210	2.022	1.987	1.643	1.625	1.281	1.029	1.377	1.002	1.295	1.677	1.559	1.589	0.833
Mg	3.192	3.221	1.903	2.199	2.521	2.936	2.423	2.680	2.890	2.815	3.588	2.761	2.412	2.604	2.577	3.650
Ca_A	0	0	0	0	0	0	0	0	0	0	0	0	0	0	0	0
Ca_B	0.100	0.103	1.807	1.794	1.823	1.730	1.826	1.872	1.850	1.711	1.722	1.647	1.538	1.536	1.545	1.710
Na_A	0.003	0.001	0.221	0.145	0.058	0.056	0.229	0.185	0.112	0.131	0.054	0.145	0.250	0.224	0.236	0.040
Na_B	0.041	0.064	0.103	0.110	0.057	0.055	0.093	0.068	0.080	0.128	0.053	0.141	0.242	0.217	0.228	0.039
K_A	0	0.005	0.004	0	0	0	0.183	0.099	0.069	0.057	0.018	0.157	0.187	0.162	0.157	0.011
Spec.	CUM	CUM	FeHB	MgHB	ACT	ACT	MgHB	MgHB	MgHB	MgHB	ACT	MgHB	MgHB	MgHB	MgHB	ACT